Concurrent design optimization of powertrain component modules in a family of electric vehicles

Applied Energy 379 (2025) 124840

Contents lists available at ScienceDirect

Applied Energy

journal homepage: www.elsevier.com/locate/apenergy

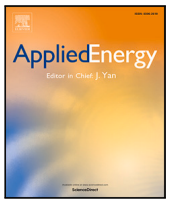

Concurrent design optimization of powertrain component modules in a family of electric vehicles☆

Maurizio Clemente *, Mauro Salazar, Theo Hofman

Department of Mechanical Engineering, Eindhoven University of Technology, Groene Loper, Eindhoven, 5600MB, The Netherlands

ARTICLE INFO

Keywords:
Electric vehicles
Design methodologies
Powertrain design
Convex optimization
Product family design
Concurrent design optimization

ABSTRACT

We present a modeling and optimization framework to design powertrains for a family of electric vehicles, focusing on the concurrent sizing of their motors and batteries. Whilst tailoring these component modules to each individual vehicle type can minimize energy consumption, it can result in high production costs due to the variety of component modules to be realized for the family of vehicles, driving the Total Costs of Ownership (TCO) high. Against this backdrop, we explore modularity and standardization strategies whereby we jointly design unique motor and battery modules to be installed in all the vehicles in the family, using a different number of these modules when needed. Such an approach results in higher production volumes of the same component module, entailing significantly lower manufacturing costs due to Economy-of-Scale (EoS) effects, and hence a potentially lower TCO for the family of vehicles. To solve the resulting "one-size-fits-all" problem, we instantiate a nested framework consisting of an inner convex optimization routine which jointly optimizes the modules' sizes and the powertrain operation of the entire family, for given driving cycles and modules' multiplicities. Likewise, we devise an outer loop comparing each configuration to identify the minimum-TCO solution with global optimality guarantees. Finally, we showcase our framework on a case study for the Tesla vehicle family in a benchmark design problem, considering the Model S, Model 3, Model X, and Model Y. Our results show that, compared to an individually tailored design, the application of our concurrent design optimization framework achieves a significant reduction of the production costs for a minimal increase in operational costs, ultimately lowering the family TCO in the benchmark design problem by 3.5%. Moreover, our concurrent design optimization methodology can reduce the TCO by up to 17% for the market conditions considered in our sensitivity study.

1. Introduction

The wider diffusion of Battery Electric Vehicles (BEVs) is considered a key objective in the transition to more sustainable mobility [1]. As a matter of fact, BEVs are important tools in the fight against pollution in cities, lowering the environmental impact by significantly decreasing particulate matter [2] and CO_2 emissions [3]. Despite the efforts in promoting policies oriented to the purchase and use of BEVs [4], they still account for a small share of the total amount of vehicles due to a relatively higher price when compared to their conventional, fossil-fuel-powered counterparts [5]. The considerable upfront cost, combined with supply shortages affecting manufacturing [6], prevents the adoption of this technology by a larger share of the general public [3,7]. In order to accelerate the transition to electric mobility, the TCO of BEVs must be reduced. Many companies have adopted design strategies aimed at developing remarkably efficient tailor-made designs [8]. However, these design choices imply considerable production costs, due to the highly specific components that are individually tailored to each vehicle model.

Conversely, it is possible to reduce production costs by leveraging Economy-of-Scale (EoS) strategies, whereas increasing the amount of identical components produced reduces their specific production cost. However, this kind of approach requires large production volumes of the same item, involving a critical manufacturing ramp-up [9] and hindering diversification, pivotal to satisfying the wide range of customer needs. We aim to address these issues by investigating a module-based product family design approach (Fig. 1) to take full advantage of the EoS strategies, substantially lowering the vehicles' TCO without limiting product diversification. Nevertheless, the mere identification

☆ This publication is part of the project NEON with project number 17628 of the research program Crossover which is (partly) financed by the Dutch Research Council (NWO).

* Corresponding author.
E-mail address: m.clemente@tue.nl (M. Clemente).

https://doi.org/10.1016/j.apenergy.2024.124840
Received 16 May 2024; Received in revised form 16 October 2024; Accepted 2 November 2024
Available online 22 November 2024

Nomenclature

α	Quadratic Motor Loss Coefficient
β	Linear Motor Loss Coefficient
η_{gb}	Gearbox Efficiency
η_{inv}	Inverter Efficiency
γ	Gear Ratio
λ_{b}	Economy-of-scale Battery Coefficients
λ_{m}	Economy-of-scale Motor Coefficients
ω_{r}	Rated Motor Speed
$\overline{E}_{\mathrm{b},0}$	Full Reference Battery Capacity
$\overline{P}_{\mathrm{m},0}$	Peak Reference Motor Power
$\overline{T}_{\mathrm{m},0}$	Maximum Reference Motor Torque
θ	Road Slope
ξ	State-of-charge
A_{f}	Frontal Area
a_k	Linear Battery Loss Coefficient
b_k	Constant Battery Loss Coefficient
C_{a}	Vehicle Acquisition Price
C_{b}	Battery Cost
c_{b}	Capacity-specific Battery Cost
c_{e}	Energy Cost
C_{g}	Glider Cost
C_{m}	Motor Cost
c_{m}	(Peak) Power-specific Motor Cost
C_{op}	Vehicle Operation Cost
C_{p}	Vehicle Production Cost
c_{r}	Drag Coefficient
c_{r}	Rolling Resistance Coefficient
d_{r}	Driving Range
$d_{\mathrm{v,lt}}$	Vehicle Lifetime
E_{b}	Battery Module Energy
E_{tot}	Overall Battery Energy
E_{v}	Vehicle Lifetime Energy Consumption
F_{v}	Distance-specific Energy Consumption
g	Gravitational Constant
J_{TCO}	Family Total Cost of Ownership
j_{TCO}	Vehicle Total Cost of Ownership
k_{oh}	Overhead Cost Factor
$m_{\mathrm{b},0}$	Reference Battery Mass
m_{d}	Driver Mass
m_{g}	Glider Mass
$m_{\mathrm{m},0}$	Reference Motor Mass
m_{p}	Payload Mass
N	Vehicle Types
N_{b}	Battery Multiplicity
N_{m}	Motor Multiplicity
N_{v}	Vehicle Production Volume
P_0	Constant Motor Loss Coefficient
P_{ac}	Motor Input Power
P_{aux}	Auxiliaries Power
P_{b}	Battery Output Power
P_{i}	Battery Internal Power
P_{m}	Motor Output Power
P_{sc}	Battery Short Circuit Power
P_{v}	Driving Cycle Required Power
r_{AWD}	All Wheel Drive Regen. Braking Fraction
r_{FWD}	Front Wheel Drive Regen. Braking Fraction
r_{w}	Wheel Radius
S_{b}	Battery Scaling Factor
S_{m}	Motor Scaling Factor
t_{a}	Acceleration Time
v_{f}	Final speed after Acceleration
v_{m}	Uphill-driving speed
v_{t}	Top Speed
w_i	Optimization Weight of the Vehicle

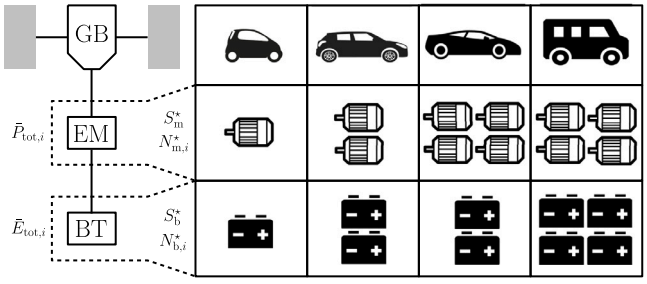

Fig. 1. Family of battery electric vehicles designed leveraging a shared modular powertrain. Every vehicle type is equipped with $N^\star_{\mathrm{m},i}$ motor modules (EM) of size $S^\star_{\mathrm{m}}$ and $N^\star_{\mathrm{b},i}$ battery modules of size $S^\star_{\mathrm{b}}$, for a total maximum motor power of $\overline{P}_{\mathrm{tot},i}$ and maximum energy capacity of $\overline{E}_{\mathrm{tot},i}$.

of a feasible design of a standardized powertrain module for multiple vehicles is a challenging task, which may result in excessive performance deterioration in the vehicles [10]. For this reason, we resort to the application of numerical optimization to find the shared size and number of modules that every vehicle is equipped with (*multiplicity*), jointly optimized to minimize the TCO of the family instead of being individually tailored for every vehicle. Against this backdrop, this paper presents the concurrent design optimization framework shown in Fig. 2 to jointly optimize the size and multiplicity of shared battery and Electric Motor (EM) modules with the operations of a family of BEVs.

Related Literature: This paper pertains to two main research lines: multi-product design and powertrain design optimization. Multi-product design is a design strategy leveraging commonality, modularity and standardization among products to reduce components' costs, provide operational and logistical advantages in part sourcing, and quality control [11]. Moreover, it fosters the development and upgrade of differentiated products efficiently, increases flexibility and responsiveness in manufacturing processes [12], and generates substantial savings in research, testing, interface design, and integration [13]. Multi-product design consists of two main processes: platform design and product family design. The former entails the development of a product platform (consisting of a common product architecture, shared physical components and processes) from the company objectives and market research. The latter accounts for the design of products starting from the common platform. Industrial players have widely studied and employed these methodologies for different products to provide cost-effective variety and customization [14]: from the Sony Walkman [15,16] to aircraft [17,18] and spacecraft [19]. The automotive sector was perhaps one of the fields where multi-product design achieved the best results. Industrial giants like Volkswagen [20,21] saved billions of dollars per year producing some of the most successful automotive platforms. In fact, "in the 1990s, automotive manufacturers that employed a platform-based product development approach gained

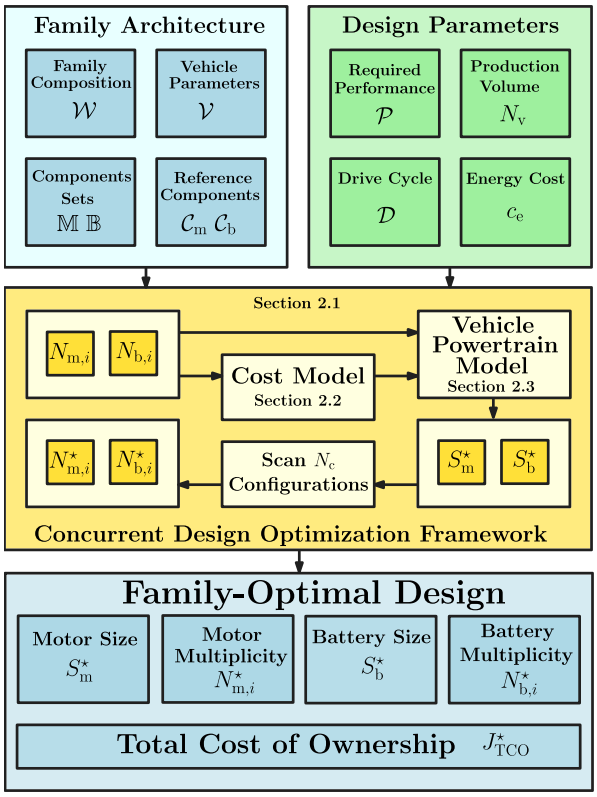

Fig. 2. Concurrent design optimization methodology diagram.

a 5.1% market share per year while those that did not, lost 2.2%" [22]. However, the application of these strategies to electric vehicles has been delayed due to the smaller production volumes compared to conventional vehicles [1], the lack of standardization [23], and the challenges in design due to the delayed ripening technology.

The second research stream concerns powertrain design optimization. This discipline has been thoroughly studied over the years, producing a considerable number of methods and applications [24]. In the last decade, powertrain design in BEVs has witnessed significant developments due to the blossoming of new system-level design optimization strategies [25,26] involving higher complexity and larger design spaces [27,28]. There are many examples of design strategies focusing on the joint optimization of the system and controls, aiming at reducing energy consumption [29–35], thus driving down the operation costs of the vehicle. Other authors analyzed the trade-off between the components' cost and the vehicle's energy efficiency [36], concluding that they are conflicting objectives in the optimization. Nevertheless, none of these methods considers the trade-off between the energy efficiency of a vehicle-tailored design against the significant manufacturing cost reduction prompted by designing shared modules serving a whole family of vehicles. The application of product family design concepts to hybrid electric vehicles can be found in one recent paper [37], where the author proposed a tool to compare different topologies and sizes from a predefined set to minimize the costs for the manufacturer. However, the algorithm can only compare a limited number of size values from predefined sets for each component in the powertrain, and the cost model does not consider the savings owing to the EoS effects. Although the concept of modular design, the use of an optimization approach, and convex optimization techniques are not new in themselves, to the best of the authors' knowledge, there are no product family design optimization frameworks for electric powertrains capturing the impact of the EoS with global optimality guarantees.

Statement of Contribution: In this paper, we reconsider the traditional vehicle-tailored optimal design methodology for BEVs in favor of a uniquely sized family-optimal module design, seeking the best compromise between the cost reduction induced by the EoS and energy efficiency. In particular, we instantiate a nested framework jointly optimizing the battery and EM modules' size and multiplicity with vehicles' operations to minimize the family TCO, explicitly accounting for the effects of production volumes. To this end, we develop:

- A cost model estimating the vehicle's TCO by capturing the influence of production volumes, energy cost, and modules' size and multiplicity;
- A vehicle and powertrain operation model, including scalable EM and battery modules, taking into account changing modules' sizing and multiplicities;
- A low-level convex optimization routine, jointly optimizing the sizing of the modules with the vehicles' operations to minimize the family TCO;
- A high-level algorithm exploring all the vehicles' multiplicity configurations of the family, each with its own optimized modules' size, to identify the one globally minimizing the overall TCO.

A preliminary version of this paper [38] was presented at the IFAC Symposium on Advances in Automotive Control in 2022. This extended version includes a broader literature review, considers a transmission in the vehicle model, introduces a cost model explicitly accounting for the effect of production volumes, and allows for the optimization of the modules' multiplicity together with their sizing. Furthermore, we present a real-world case study considering a leading manufacturer vehicle family, and a sensitivity study on the impact of energy costs and vehicles' production volumes on the optimal design solution. In this benchmark problem, we assumed the same type fraction for each vehicle to demonstrate our BEV design framework independently of the sales reported by the specific company.

Organization: The remainder of this paper is organized as follows: Section 2 introduces the concurrent optimization design methodology, describes the vehicle's cost and powertrain models, frames the optimization problem formulation, and discusses the assumptions and limitations of our approach. In Section 3, we demonstrate the applications of our framework with a benchmark problem where we identify the optimal modules' size and multiplicity for the Tesla vehicle family. Furthermore, we produce a sensitivity analysis of the methodology advantages under different energy costs and production volumes. The conclusions are drawn in Section 4, together with an outlook on future research.

2. Methodology

In this section, we illustrate our framework in detail. Section 2.1 describes the concurrent design optimization problem, while Sections 2.2 and 2.3 characterize the cost and powertrain model, respectively. Finally, we formalize the optimization problem formulation in Section 2.4 and discuss the assumptions and limitations of our approach in Section 2.5.

2.1. Problem definition: Concurrent design optimization

The traditional powertrain design approach consists of tailoring the components' sizes to each individual vehicle. When considering electric vehicles, the large high-efficiency area in an EM torque map allows for merely small power losses in many different operating points, as opposed to the conventional internal combustion engine's relatively tight sweet spot region (Fig. 3). This feature enables differently-sized vehicles to share the same motor model with limited drawbacks, which can be further reduced when employing a modular design, taking advantage of the topologies enabled by the technology. Furthermore, the battery is an intrinsically modular component and can be easily manufactured in packs of the family-optimal size, satisfying the energy requirements with the optimal number of modules and fostering

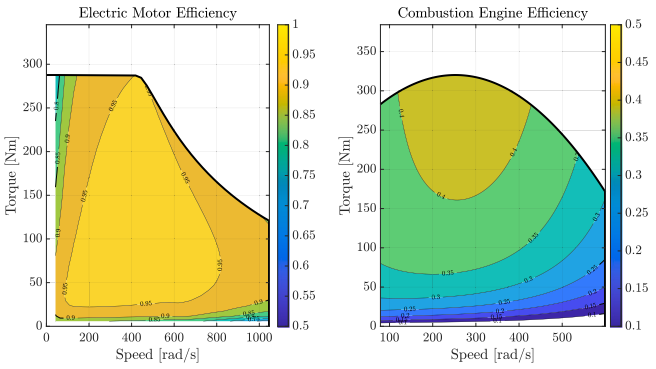

Fig. 3. Efficiency map of an electric motor (left) compared with an internal combustion engine (right).
Source: Data from [39].

customization and diversification (range-extended variants). The great advantage of using the same module type for many different vehicles lies in the EoS effects triggered by the increased production volumes. Compared to a vehicle-tailored design, where every vehicle features components specifically optimized for its design and operations, in concurrent design the manufacturer can amortize overhead costs on a larger number of items, reducing their specific cost. Although this approach enables battery and motor swapping business, our design methodology does not focus on this feature, prioritizing the cost reduction induced by standardization and modularization. However, due to the asymptotic behavior of the phenomenon, usually described as the "law of diminishing returns", an increase in production volumes will bear relatively smaller advantages in module cost every time. Despite the module cost reduction, the standardization of the components could lead to underwhelming performance or excessively high energy consumption, negatively impacting the end-user of the vehicle. For this reason, we exploit numerical optimization techniques to strike the optimal balance between energy efficiency and EoS cost reduction, taking into account all the constraints from each of the vehicles in the family simultaneously, to avoid performance degradation. We devise a bi-level, nested algorithm exploring every configuration of the modules in the family and leveraging convex properties to rapidly converge to the globally optimal solution. Subsequently, we compare the optimally sized configurations to identify the lowest TCO while retaining information on the other sub-optimal solutions.

Hereby, we present the design variables of the problem: the motor scaling factor S_{m}, the battery scaling factor S_{b}, and the respective number of modules (*multiplicity*) $N_{\mathrm{m},i}$ and $N_{\mathrm{b},i}$. The subscript i indicates that the quantity differs from one vehicle type to the other, as opposed to their common sizing. We denote the minimum and maximum value of a variable X by introducing a line below and above its symbol, $\underline{X}$ and $\overline{X}$, respectively. We devise our model using a reference motor and a reference battery for the identification of the parameters. In order to preserve a clean notation, these parameters are included in the sets of reference components $\mathcal{C}_{\mathrm{m}}$ and $\mathcal{C}_{\mathrm{b}}$

$$\mathcal{C}_{\mathrm{m}} := \left\{ P_0, \beta, \alpha, m_{\mathrm{m,o}}, \overline{P}_{\mathrm{m,o}}, \omega_{\mathrm{r}}, \gamma, r_{\mathrm{FWD}}, r_{\mathrm{AWD}} \right\},$$

$$\mathcal{C}_{\mathrm{b}} := \left\{ a_k, b_k, m_{\mathrm{b,o}}, \overline{E}_{\mathrm{b,o}}, \underline{\xi}, \overline{\xi} \right\},$$

where the motor loss coefficients P_0, β, and α are dependent on the motor speed ω and subject to identification. Similarly, the battery loss coefficients a_k and b_k, $k \in \{1, \dots, K\}$, are identified from a reference battery and used to determine the short-circuit power P_{sc} of the battery, a measure of efficiency described in Section 2.3.5. The constants $m_{\mathrm{m,o}}$ and $m_{\mathrm{b,o}}$ are the reference masses of the motor and battery, respectively. The parameters $\underline{\xi}$ and $\overline{\xi}$ are the minimum and maximum state-of-charge operational limits, while r_{FWD} and r_{AWD} are the regenerative braking fraction for a Front-Wheel Drive and an All-Wheel Drive. Finally, γ is the gear ratio and ω_{r} is the speed at which the maximum torque and maximum power curves intersect, also called rated speed. Consistently, we assume that the vehicle's maximum output power of the motor(s) $\overline{P}_{\mathrm{tot},i}$ and the maximum energy of the battery pack $\overline{E}_{\mathrm{tot},i}$ are obtained by linearly scaling the reference motor's maximum output power $\overline{P}_{\mathrm{m,o}}$ and reference battery maximum energy capacity $\overline{E}_{\mathrm{b,o}}$, taking into account the modules' multiplicity

$$\overline{P}_{\mathrm{tot},i} = S_{\mathrm{m}} \cdot N_{\mathrm{m},i} \cdot \overline{P}_{\mathrm{m,o}}, \tag{1}$$

$$\overline{E}_{\mathrm{tot},i} = S_{\mathrm{b}} \cdot N_{\mathrm{b},i} \cdot \overline{E}_{\mathrm{b,o}}. \tag{2}$$

Nonetheless, these approximations are only valid in the range of scales

$$S_{\mathrm{m}} \in \left[\underline{S}_{\mathrm{m}}, \overline{S}_{\mathrm{m}} \right] \subseteq \mathbb{R}_+, \tag{3}$$

$$S_{\mathrm{b}} \in \left[\underline{S}_{\mathrm{b}}, \overline{S}_{\mathrm{b}} \right] \subseteq \mathbb{R}_+, \tag{4}$$

while the possible multiplicities of the modules in the vehicles are listed in the sets $\mathbb{M}, \mathbb{B}$

$$N_{\mathrm{m},i} \in \mathbb{M} := \left\{ \underline{N}_{\mathrm{m}}, \dots, \overline{N}_{\mathrm{m}} \right\} \subseteq \mathbb{N}_+, \tag{5}$$

$$N_{\mathrm{b},i} \in \mathbb{B} := \left\{ \underline{N}_{\mathrm{b}}, \dots, \overline{N}_{\mathrm{b}} \right\} \subseteq \mathbb{N}_+. \tag{6}$$

Moreover, we introduce the Family Composition $\mathcal{W}$ and Vehicle Parameters $\mathcal{V}$ sets from the Family Architecture block of Fig. 2,

$$\mathcal{W} := \{ w_1, w_2, \dots, w_i \},$$

$$\mathcal{V}_i := \{ m_{\mathrm{g},i}, m_{\mathrm{p},i}, m_{\mathrm{d},i}, \eta_{\mathrm{gb}}, \eta_{\mathrm{inv}}, r_{\mathrm{w},i}, c_{\mathrm{r},i}, c_{\mathrm{d},i}, A_{\mathrm{f},i}, P_{\mathrm{aux}} \} \subseteq \mathcal{V},$$

where the w_i are the fractions of the total number of vehicles N_{v} of the ith type, while the set $\mathcal{V}$ includes N subsets $\mathcal{V}_i$, one for each vehicle type considered. Each subset $\mathcal{V}_i$ contains, in respective order, the glider mass $m_{\mathrm{g},i}$, the payload mass $m_{\mathrm{p},i}$, the gearbox efficiency η_{gb}, the inverter efficiency η_{inv}, the wheel radius $r_{\mathrm{w},i}$, the frontal area $A_{\mathrm{f},i}$, and the rolling resistance $c_{\mathrm{r},i}$ and aerodynamic drag $c_{\mathrm{d},i}$ coefficients. Furthermore, we include the required performance that the vehicle has to satisfy in the set $\mathcal{P}$, with its N subsets

$$\mathcal{P}_i := \left\{ \bar{t}_{\mathrm{a},i}, v_{\mathrm{f}}, \underline{v}_{\mathrm{t},i}, \underline{d}_{\mathrm{r},i}, \underline{v}_{\mathrm{m},i}, \underline{\theta}_i \right\} \in \mathcal{P},$$

where $\bar{t}_{\mathrm{a},i}$ is the maximum time needed to accelerate from 0 to v_{f}, $\underline{v}_{\mathrm{t},i}$ the minimum required top speed, $\underline{d}_{\mathrm{r},i}$ the minimum required range, $\underline{v}_{\mathrm{m},i}$ is the minimum speed at which the vehicle shall be able to drive facing a slope of at least $\underline{\theta}_i$.

Ultimately, using our concurrent design optimization framework, we are able to identify the family-optimal sizes $S^\star_{\mathrm{m}}, S^\star_{\mathrm{b}}$ and multiplicities $N^\star_{\mathrm{m},i}, N^\star_{\mathrm{b},i}$ of the modules minimizing the family TCO $J^\star_{\mathrm{TCO}}$ by striking the optimal compromise between production and operational costs.

2.2. Cost model

The majority of authors who developed a cost model for BEVs predominantly analyze the decline in costs over time. These analyses are based on technology-development predictions, which are affected by a high degree of uncertainty [40–45]. Conversely, we introduce a more robust model based on the relation between cost of motors and batteries and production volumes instead of uncertain technology development forecasts. For this reason, we identified the asymptotic dependence of the components' cost on the production volume from manufacturing data [41,42,46–52], and validated with data from the market [53–61].

We introduce an asymptotic dependence of the components' cost on the production volume, based on manufacturing data, to account for the impact of EoS effects. We display the data used in Table A.6 of Appendix A: First, we portray the asymptotic curves resulting from Eqs. (14) and (16) from Section 2.2.2 (Motor Cost) and Section 2.2.3 (Battery Cost) in Figs. A.9 (motor) and A.10 (battery pack). Then, we validate the results of the cost model in Table A.7, providing a visual representation in Fig. A.11. However, we do not claim any correlation of production cost with sales, as this relation depends on the analysis of complicated customer-market dynamics which are beyond the scope of this paper. In our concurrent design optimization methodology, the description of these effects enables analyzing the trade-off in TCO between a tailored design, where the components have larger production costs and higher efficiencies, and a family-shared design, with smaller costs and lower efficiencies. For the purpose of this paper, we assume fixed or vehicle-class dependent costs such as insurance, maintenance, and taxes to be independent of the decision variables in the optimization framework [47]. While these additional costs could be readily included in the model, the minor differences in motor and battery sizing compared to the (individual) vehicle-tailored design do not significantly affect the relative outcome of our study. For this reason, in a first approximation, we disregard them in our analysis. Hereby, we define the family TCO as the sum of the TCOs of all the vehicles in the family $j_{\mathrm{TCO},i}$:

$$J_{\mathrm{TCO}} = \sum_{i=1}^{N} w_i \cdot j_{\mathrm{TCO},i}. \tag{7}$$

Each vehicle's TCO is composed of two main contributions: vehicle acquisition price $C_{\mathrm{a},i}$ and operation cost $C_{\mathrm{op},i}$

$$j_{\mathrm{TCO},i} = C_{\mathrm{a},i} + C_{\mathrm{op},i}, \tag{8}$$

where $C_{\mathrm{a},i}$ can be related to the production costs $C_{\mathrm{p},i}$ by means of a fixed overhead costs percentage k_{oh} [62,63], as displayed in Fig. A.12

$$C_{\mathrm{a},i} = \frac{C_{\mathrm{p},i}}{k_{\mathrm{oh}}}, \tag{9}$$

while the operation costs are computed by multiplying the lifelong vehicle energy consumption $E_{\mathrm{v},i}$ and the energy cost c_{e},

$$C_{\mathrm{op},i} = E_{\mathrm{v},i} \cdot c_{\mathrm{e}}. \tag{10}$$

In turn, $E_{\mathrm{v},i}$ is computed from the distance-specific energy consumption $F_{\mathrm{v},i}$ from the powertrain model in Section 2.3 and the vehicle lifetime $d_{\mathrm{v,lt}}$ expressed as a distance

$$E_{\mathrm{v},i} = F_{\mathrm{v},i} \cdot d_{\mathrm{v,lt}}. \tag{11}$$

The vehicle production cost can be divided further into different contributions owing to the glider C_{g}, motors C_{m}, and battery pack C_{b}

$$C_{\mathrm{p},i} = C_{\mathrm{g},i} + C_{\mathrm{m},i} + C_{\mathrm{b},i}. \tag{12}$$

2.2.1. Glider cost

The glider comprises the body, chassis, low-voltage electrical components, exterior, and interior [45,64]. We also include the cost of the gearbox in the glider, as we assume it is not influenced by the production volumes [65]. For the context of our analysis, and without loss of generality, we will consider the glider's cost a constant term depending exclusively on the vehicle class [42]. On the other hand, motor and battery costs are functions of the modules' size, multiplicity on the specific vehicle, and production volumes.

2.2.2. Motor cost

We consider the motor module cost to scale linearly with its peak power $\overline{P}_{\mathrm{m}}$, following several studies [43,44,47,49,66,67]. Hence, depending on the number of modules the vehicle is equipped with, the total production cost of the motors becomes

$$C_{\mathrm{m},i} = c_{\mathrm{m}} \cdot S_{\mathrm{m}} \cdot N_{\mathrm{m},i} \cdot \overline{P}_{\mathrm{m,o}}, \tag{13}$$

where c_{m} is the (peak) power-specific motor cost and is composed of two terms

$$c_{\mathrm{m}} = c_{\mathrm{m},y} + \frac{\lambda_{\mathrm{m},1}}{(N_{\mathrm{m},i} \cdot N_{\mathrm{v}} \cdot N - 1)^{\lambda_{\mathrm{m},2}}}. \tag{14}$$

The first term $c_{\mathrm{m},y}$ includes all the costs independent of volumes, like materials and process efficiency, indirectly depending on the market and technology level, which varies every year [46]. The second term takes into account the effect of the EoS. For this contribution, we use an asymptotic fit to reckon all the costs that can be amortized on a variable number of produced items N_{v}. The coefficients $\lambda_{\mathrm{m},1}$ and $\lambda_{\mathrm{m},2}$ are subject to identification, as reported in Appendix A.

2.2.3. Battery cost

The battery pack is one of the most expensive parts of an electric vehicle's powertrain [43]. We assume its cost to linearly scale with the maximum battery module capacity

$$C_{\mathrm{b},i} = c_{\mathrm{b}} \cdot S_{\mathrm{b}} \cdot N_{\mathrm{b},i} \cdot \overline{E}_{\mathrm{b,o}}, \tag{15}$$

where c_{b} is the capacity-specific cost and it is composed of two terms, in a similar fashion to the motor model

$$c_{\mathrm{b}} = c_{\mathrm{b},y} + \frac{\lambda_{\mathrm{b},1}}{(N_{\mathrm{b},i} \cdot N_{\mathrm{v}} \cdot N - 1)^{\lambda_{\mathrm{b},2}}}, \tag{16}$$

where the coefficients $\lambda_{\mathrm{b},1}$ and $\lambda_{\mathrm{b},2}$ of the asymptotic term are identified from data available in the literature, as shown in Appendix A.

2.3. Vehicle powertrain model

In this section, we describe the equations employed to model the powertrain behavior. In accordance with common practices in this field [24,68], we apply a quasi-static modeling technique to predict the components' behavior and estimate the distance-specific energy consumption. This formulation allows for the identification of the family-optimal modules' sizes for every configuration of modules in the family, accounting for their impact on energy consumption while still preserving convexity and its properties. Fig. 4 displays the vehicle powertrain model as well as the cost model described in Section 2.2, showing inputs, outputs, and interconnections. Section 2.3.1 presents the vehicle's longitudinal dynamics, and Section 2.3.2 gives insights into the mass model, taking into account the modules' size and number. Section 2.3.4 introduces the EM model, whilst Section 2.3.5 refers to the battery pack, and Section 2.3.6 presents the required performance constraints that the vehicles need to satisfy. For the sake of simplicity, we drop dependence on time t whenever it is clear from the context. Finally, even though we included extra passages in the derivation of some equations to facilitate understanding for the reader, we only label the version included in the formulation of Problem 1 **(Concurrent Design Optimization Problem)** to avoid redundancy and maintain a clear mathematical definition of the problem.

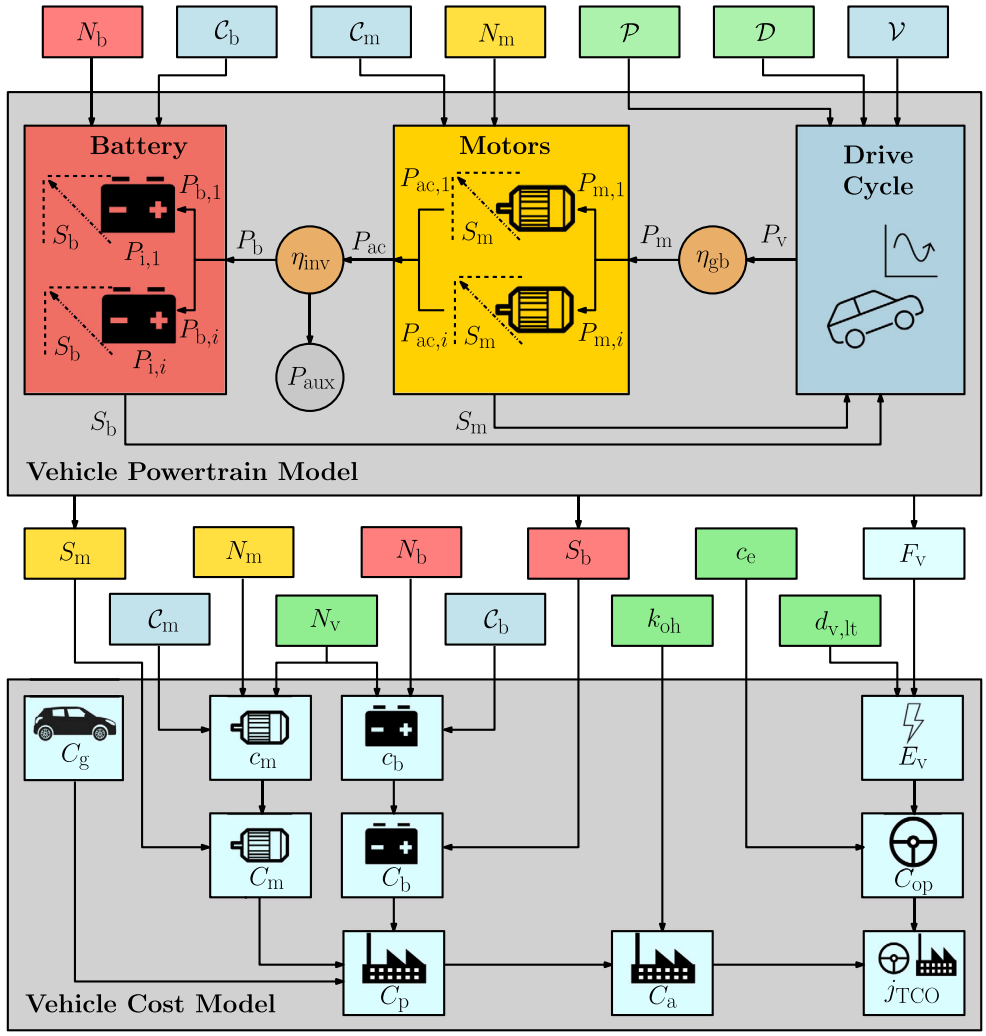

Fig. 4. Flow diagram explaining the algorithm employed in computing the objective function (TCO) of our concurrent design optimization framework.

2.3.1. Longitudinal dynamics

We optimize the design of the vehicles for a given driving cycle $\mathcal{D}$ of length d with exogenous longitudinal speed, acceleration, and slope trajectories $v(t)$, $a(t)$, and $\theta(t)$. Hence, the required power at the wheels P_{v} can be expressed as

$$P_{\mathrm{v},i} = m_i \cdot v \cdot \left(c_{\mathrm{r},i} \cdot g \cdot \cos(\theta) + g \cdot \sin(\theta) + a\right) + \frac{1}{2} \cdot \rho \cdot c_{\mathrm{d},i} \cdot A_{\mathrm{f},i} \cdot v^3, \quad (17)$$

where m_i is the total mass of each vehicle, g is the gravitational acceleration, ρ is the density of the air, $c_{\mathrm{d},i}$ is the aerodynamic drag coefficient, and $c_{\mathrm{r},i}$ is the rolling resistance coefficient.

2.3.2. Mass

The vehicle's mass m_i consists of several contributions: the glider mass $m_{\mathrm{g},i}$, the constant driver mass m_{d}, the payload mass $m_{\mathrm{p},i}$, and the motor and battery mass, computed by scaling $m_{\mathrm{m,o}}$ and $m_{\mathrm{b,o}}$, accounting for the number of modules

$$m_i = m_{\mathrm{g},i} + m_{\mathrm{d}} + m_{\mathrm{p},i} + m_{\mathrm{m,o}} \cdot S_{\mathrm{m}} \cdot N_{\mathrm{m},i} + m_{\mathrm{b,o}} \cdot S_{\mathrm{b}} \cdot N_{\mathrm{b},i}. \quad (18)$$

2.3.3. Transmission

We assume the regenerative braking system always in function when the power required at the wheels P_{req} is negative and it is equally divided among the N_{m} motor modules through fixed-gear transmissions (Fig. 5), whereby we consider the gear ratio γ specifically designed for the motor speed interval considered. The transmissions introduce losses that we model via a constant efficiency η_{gb}:

$$P_{\mathrm{m},i} = \begin{cases} \frac{P_{\mathrm{v},i}}{\eta_{\mathrm{gb}} \cdot N_{\mathrm{m},i}} & \text{if } P_{\mathrm{req},i} \geq 0 \\ r_{\mathrm{b},i} \cdot \frac{\eta_{\mathrm{gb}} \cdot P_{\mathrm{v},i}}{N_{\mathrm{m},i}} & \text{if } P_{\mathrm{req},i} < 0, \end{cases}$$

$$r_{\mathrm{b},i} = \begin{cases} r_{\mathrm{FWD}} & \text{if FWD} \\ r_{\mathrm{AWD}} & \text{if AWD}, \end{cases}$$

where the regenerative braking fraction r_{b} accounts for the braking capabilities of the vehicle's topology r_{FWD} and r_{AWD}, included in the set $\mathcal{C}_{\mathrm{m}}$. This fraction only determines the maximum amount of power that can be recuperated based on the axles linked to a recuperation device, while the effective power regenerated depends on the efficiency of the motor(s) at that specific operating point. We can relax this constraint to an inequality without changing the problem solution (lossless relaxation) as

$$P_{\mathrm{m},i} \geq \frac{P_{\mathrm{v},i}}{\eta_{\mathrm{gb}} \cdot N_{\mathrm{m},i}}, \quad (19)$$

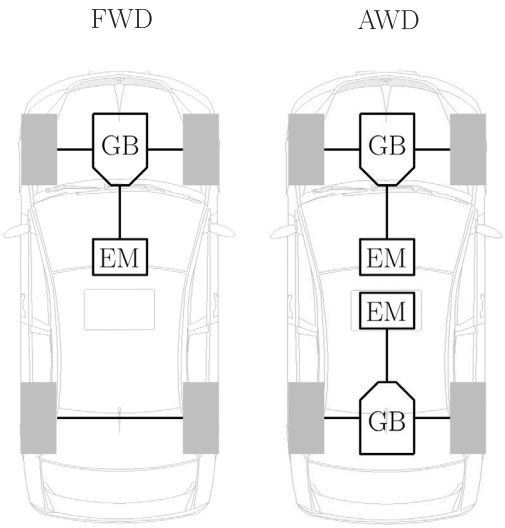

Fig. 5. Vehicle topologies considered in this framework: Front-wheel drive (FWD) for vehicles equipping one motor module, and All-wheel drive (AWD) for two.

$$P_{\mathrm{m},i} \geq r_{\mathrm{b},i} \cdot \frac{\eta_{\mathrm{gb}} \cdot P_{\mathrm{v},i}}{N_{\mathrm{m},i}}. \tag{20}$$

In fact, thanks to the particular problem structure, the optimal solution is located on the boundary, implying that these constraints will always hold with equality [69]. Ultimately, assuming any value higher than the strictly necessary would be sub-optimal since it would entail higher losses and thus additional costs.

2.3.4. Electric motor

Analogously to our previous work [38], we make use of a second-order polynomial approximation of the reference motor losses $P_{\mathrm{m,o,loss}}$, extending a quadratic approximation [68] to retain accuracy, without losing convexity

$$P_{\mathrm{m,o,loss}} = P_0(\omega) + \beta(\omega) \cdot P_{\mathrm{m,o}} + \alpha(\omega) \cdot P_{\mathrm{m,o}}^2.$$

Furthermore, we assume that the operational limits $\underline{P}_{\mathrm{m,o}}$ and $\overline{P}_{\mathrm{m,o}}$ scale linearly with respect to the reference values

$$P_{\mathrm{m},i} \in \left[\underline{P}_{\mathrm{m,o}}, \overline{P}_{\mathrm{m,o}}\right] \cdot S_{\mathrm{m}}. \tag{21}$$

Following the same rationale, we can write $P_{\mathrm{m,loss}}$ for every motor module as

$$P_{\mathrm{m,loss},i} = \left(P_0(\omega) + \beta(\omega) \cdot \frac{P_{\mathrm{m},i}}{S_{\mathrm{m}}} + \alpha(\omega) \cdot \frac{P_{\mathrm{m},i}^2}{S_{\mathrm{m}}^2}\right) \cdot S_{\mathrm{m}},$$

yielding

$$P_{\mathrm{m,loss},i} = P_0(\omega) \cdot S_{\mathrm{m}} + \beta(\omega) \cdot P_{\mathrm{m},i} + \alpha(\omega) \cdot \frac{P_{\mathrm{m},i}^2}{S_{\mathrm{m}}}.$$

Finally, we obtain the AC input motor power $P_{\mathrm{ac},i}$ equation

$$P_{\mathrm{ac},i} = \left(P_{\mathrm{m},i} + P_{\mathrm{m,loss},i}\right),$$

and we replace the expression for the losses

$$P_{\mathrm{ac},i} = P_{\mathrm{m},i} + P_0(\omega) \cdot S_{\mathrm{m}} + \beta(\omega) \cdot P_{\mathrm{m},i} + \alpha(\omega) \cdot \frac{P_{\mathrm{m},i}^2}{S_{\mathrm{m}}}.$$

Analogously to what has been done in Eq. (19), this equation can be losslessly relaxed for the purpose of retaining convexity [70], obtaining the second-order conic constraint

$$\left(P_{\mathrm{ac},i} - P_{\mathrm{m},i} - S_{\mathrm{m}} \cdot P_0(\omega) - \beta(\omega) \cdot P_{\mathrm{m},i}\right) + \frac{S_{\mathrm{m}}}{\alpha(\omega)} \geq$$

$$\left\| \begin{matrix} 2 \cdot P_{\mathrm{m},i} \\ \left(P_{\mathrm{ac},i} - P_{\mathrm{m},i} - S_{\mathrm{m}} \cdot P_0(\omega) - \beta(\omega) \cdot P_{\mathrm{m},i}\right) - \frac{S_{\mathrm{m}}}{\alpha(\omega)} \end{matrix} \right\|_2. \tag{22}$$

2.3.5. Battery

Similarly to what has been implemented for the EM, for each vehicle of the ith type, every module's output battery power $P_{\mathrm{b},i}$ can be found starting from $P_{\mathrm{ac},i}$ by considering the inverter efficiency η_{inv}, power consumption of auxiliary systems $P_{\mathrm{aux},i}$ (heating, air conditioning, lights, etc.), and motor and battery modules' multiplicity $N_{\mathrm{m},i}$ and $N_{\mathrm{b},i}$. Following the assumption that every module supplies an equal amount of output power in the ith vehicle,

$$P_{\mathrm{b},i} = \begin{cases} \frac{1}{N_{\mathrm{b},i}} \cdot \left(\frac{P_{\mathrm{ac},i} \cdot N_{\mathrm{m},i}}{\eta_{\mathrm{inv}}} + P_{\mathrm{aux},i}\right) & \text{if } P_{\mathrm{ac},i} \geq 0 \\ \frac{1}{N_{\mathrm{b},i}} \cdot \left(\eta_{\mathrm{inv}} \cdot P_{\mathrm{ac},i} \cdot N_{\mathrm{m},i} + P_{\mathrm{aux},i}\right) & \text{if } P_{\mathrm{ac},i} < 0, \end{cases}$$

that can be relaxed to

$$P_{\mathrm{b},i} \geq \frac{1}{N_{\mathrm{b},i}} \cdot \left(\frac{P_{\mathrm{ac},i} \cdot N_{\mathrm{m},i}}{\eta_{\mathrm{inv}}} + P_{\mathrm{aux},i}\right), \tag{23}$$

$$P_{\mathrm{b},i} \geq \frac{1}{N_{\mathrm{b},i}} \cdot \left(\eta_{\mathrm{inv}} \cdot P_{\mathrm{ac},i} \cdot N_{\mathrm{m},i} + P_{\mathrm{aux},i}\right). \tag{24}$$

We model the battery's internal losses using a function of the power that the battery would release when short-circuited: the "short circuit power" [38] $P_{\mathrm{sc},i}$. We make use of a convex piece-wise affine approximation of the function composed of K parts, depending on the energy $E_{\mathrm{b},i}$ and size S_{b} [68]. Hence, for every battery module,

$$P_{\mathrm{i},i} = P_{\mathrm{b},i} + \frac{P_{\mathrm{i},i}^2}{P_{\mathrm{sc},i}},$$

where

$$P_{\mathrm{sc},i} = \min_{k \in \{1,\ldots,K\}} \left\{a_k \cdot E_{\mathrm{b},i} + b_k \cdot S_{\mathrm{b}}\right\}.$$

However, the form of this constraint would not allow a convex formulation, therefore, we apply a lossless relaxation to treat a set of affine inequalities.

$$P_{\mathrm{sc},i} \leq a_k \cdot E_{\mathrm{b},i} + b_k \cdot S_{\mathrm{b}} \; \forall k. \in \{1, \ldots, K\}. \tag{25}$$

Following the same logic applied in Section 2.3.4, we also relax the battery losses equation to

$$\left(P_{\mathrm{i},i} - P_{\mathrm{b},i}\right) + P_{\mathrm{sc},i} \geq \left\| \begin{matrix} 2 \cdot P_{\mathrm{i},i} \\ \left(P_{\mathrm{i},i} - P_{\mathrm{b},i}\right) - P_{\mathrm{sc},i} \end{matrix} \right\|_2. \tag{26}$$

The overall energy of the battery $E_{\mathrm{tot},i}$ is determined by each module's size and the total number of modules per vehicle

$$E_{\mathrm{tot},i} \in \left[\; \overline{E}_{\mathrm{b,o}} \cdot \underline{\xi}, \overline{E}_{\mathrm{b,o}} \cdot \overline{\xi} \;\right] \cdot S_{\mathrm{b}} \cdot N_{\mathrm{b},i}, \tag{27}$$

while the dynamic of $E_{\mathrm{tot},i}$ is influenced by the internal power via

$$\frac{\mathrm{d}E_{\mathrm{tot},i}}{\mathrm{d}t} = -N_{\mathrm{b}} \cdot P_{\mathrm{i},i}. \tag{28}$$

Ultimately, we evaluate the distance-specific energy consumption $F_{\mathrm{v},i}$ by dividing $E_{\mathrm{tot},i}$ by driving cycle length d

$$F_{\mathrm{v},i} = \frac{E_{\mathrm{tot},i}(0) - E_{\mathrm{tot},i}(T)}{d}. \tag{29}$$

Since we consider a variable efficiency of the battery through $P_{\mathrm{sc},i}$, we include a constraint to ensure that the operations are conducted around the half-capacity level of the battery by averaging the maximum

capacity at the start and the minimum capacity at the end of the driving cycle

$$E_{\mathrm{tot},i}(0) = S_\mathrm{b} \cdot \overline{\xi} \cdot \overline{E}_\mathrm{b,o} \cdot N_{\mathrm{b},i},$$

$$E_{\mathrm{tot},i}(T) = S_\mathrm{b} \cdot \underline{\xi} \cdot \overline{E}_\mathrm{b} \cdot N_{\mathrm{b},i},$$

$$E_{\mathrm{tot},i}(0) + E_{\mathrm{tot},i}(T) = S_\mathrm{b} \cdot \left(\overline{\xi} + \underline{\xi}\right) \cdot \overline{E}_\mathrm{b,o} \cdot N_{\mathrm{b},i}. \tag{30}$$

2.3.6. Performance constraints

Besides the equations modeling the powertrain behavior during vehicles' operations, we include constraints on the performance of each vehicle, derived from [1], to ensure that the design of every single vehicle meets all expectation set. Hence, we write in convex form the acceleration time, top speed, power gradability, torque gradability, and range constraints as

$$N_{\mathrm{m},i} \cdot S_\mathrm{m} \cdot t_{\mathrm{a},i} \leq \frac{\omega_\mathrm{r} \cdot r_{\mathrm{w},i}^2 \cdot m_i}{\overline{T}_\mathrm{m,o} \cdot \gamma^2} + \frac{m_i \cdot \left(v_\mathrm{f}^2 + \frac{\omega_\mathrm{r}^2}{\gamma^2} \cdot r_{\mathrm{w},i}^2\right)}{2 \cdot \overline{P}_\mathrm{m,o}}, \tag{31}$$

$$N_{\mathrm{m},i} \cdot S_\mathrm{m} \cdot \overline{P}_\mathrm{m,o} \geq \frac{1}{2} \cdot \rho \cdot c_{\mathrm{d},i} \cdot A_{\mathrm{f},i} \cdot \left(v_{\mathrm{t},i}\right)^3, \tag{32}$$

$$N_{\mathrm{m},i} \cdot S_\mathrm{m} \cdot \overline{P}_{\mathrm{m},o} \geq m_i \cdot g \cdot v_{\mathrm{m},i} \cdot \sin(\theta_i), \tag{33}$$

$$N_{\mathrm{m},i} \cdot S_\mathrm{m} \cdot \overline{T}_\mathrm{m,o} \cdot \gamma \geq m_i \cdot g \cdot r_{\mathrm{w},i} \cdot \sin(\theta_i), \tag{34}$$

$$E_{\mathrm{tot},i}(0) - E_{\mathrm{tot},i}(T) \leq N_{\mathrm{b},i} \cdot S_\mathrm{b} \cdot \left(\overline{\xi} - \underline{\xi}\right) \cdot \overline{E}_\mathrm{b,o} \cdot \frac{d}{d_{\mathrm{r},i}}, \tag{35}$$

where $\overline{T}_\mathrm{m,o}$ is the maximum reference torque

$$\overline{T}_\mathrm{m,o} = \frac{\overline{P}_\mathrm{m,o}}{\omega_\mathrm{r}}.$$

The values of the acceleration time $t_{\mathrm{a},i}$, top speed $v_{\mathrm{t},i}$, uphill speed $v_{\mathrm{m},i}$, slope θ_i, and range $d_{\mathrm{r},i}$ are bounded by the required performance in the set $\mathcal{P}$

$$t_{\mathrm{a},i} \leq \bar{t}_{\mathrm{a},i}, \tag{36}$$

$$v_{\mathrm{t},i} \geq \underline{v}_{\mathrm{t},i}, \tag{37}$$

$$v_{\mathrm{m},i} \geq \underline{v}_{\mathrm{m},i}, \tag{38}$$

$$\theta_i \geq \underline{\theta}_i, \tag{39}$$

$$d_{\mathrm{r},i} \geq \underline{d}_{\mathrm{r},i}. \tag{40}$$

2.4. Optimization problem formulation

We formulate the concurrent design optimization problem with the objective of minimizing the TCO of the vehicle family by choosing the sizing of the shared modules and their multiplicity as follows.

Problem 1 (*Concurrent Design Optimization Problem*)**.** Given a family of battery electric vehicles with modular powertrains, the TCO-optimal shared modules' sizes and multiplicity for the whole family are the solution of

$$\min_{S_\mathrm{m}, S_\mathrm{b}, N_{\mathrm{m},i}, N_{\mathrm{b},i}} J_\mathrm{TCO}$$
$$\text{s.t. Shared Constraints (1)–(6)}$$
$$\text{Vehicle Constraints (8)–(40)} \quad \forall k \quad \forall i$$

This problem can be solved with global optimality guarantees in a nested fashion: For given $N_{\mathrm{m},i}$ and $N_{\mathrm{b},i}$, this problem can be framed as a second-order conic program and rapidly solved to global optimality with standard algorithms. Thus, we analyze each of the N_c possible configurations

$$N_\mathrm{c} = \left(|\mathbb{M}| \cdot |\mathbb{B}|\right)^N,$$

leveraging the polynomial solving time of the convex approach, and identify the globally optimal solution through an exhaustive search.

2.5. Discussion

In this paragraph, we present some clarification on the assumptions and limitations of our work. First, we conservatively assumed that every vehicle has a fixed percentage of overhead costs, yet the methodology is still sound for every cost model incorporating the effect of EoS. Second, we scale the electric motor mass linearly as a function of the maximum power and the battery size only by acting on the number of cells in parallel, thus changing its energy without altering the battery voltage. These scaling methods are in line with high-level modeling approaches and optimal sizing design problems [71]. Third, we assume that every vehicle is equipped with the same transmission modules. The gear ratio γ is considered to be specifically designed for the motor speed range, which remains constant while linearly scaling the motor in torque. For a fair comparison, γ is kept constant both in the individual vehicle-tailored design and in the concurrent design optimization. This assumption is in accordance with the common design practice among electric vehicle manufacturers of using a standard reduction gear. Furthermore, we focus our attention on the economical aspect of the design, since it is one of the major issues preventing a larger uptake of electric mobility [3]. However, the powertrain sizing also influences the environmental aspect of BEVs. In fact, batteries place a heavy burden on the environment: Their production process influences different impact categories such as acidification, eutrophication, human toxicity, eco-toxicity, and resource depletion. Yet, the major contribution in the battery life-cycle emissions is not the production process, but, the electricity consumption during the battery's life inside the vehicle [72–74]. In our concurrent design optimization methodology, we sacrifice some energy efficiency in favor of cheaper vehicles, increasing the lifetime energy consumption (larger batteries, heavier vehicles) and possibly leading to more emissions when compared to (individual) vehicle-tailored design. Nevertheless, since even in the case of a very carbon-intense electricity mix, BEVs still outperform conventional fossil-fuel-powered vehicles in terms of emissions, increasing the share of electric vehicles directly translates into a reduction of the life cycle emissions and environmental impact. To compare the influence of each component's sizing on the overall environmental impact of the vehicle, an extended life cycle assessment would be needed, however, it is beyond the scope of our paper. Finally, we ensure the problem convexity by adopting a convex objective function and a convex domain. Every constraint included in Problem 1 delineates a convex space, and, since the intersection of convex spaces is still convex, the overall domain is convex [75]. Since the only integer variables of the problem are the motor and battery multiplicities, the problem could be solved as a Mixed Integer Second Order Conic Program (MISOCP). Nevertheless, we apply a nested approach where we solve a SOCP for every combination of the modules multiplicity in each vehicle, leveraging the fast solving time of convex programs to retain information on the other sub-optimal configurations, additionally obtaining sensitivity information.

Table 1
Cost model parameters [78–80].

Parameter	Value	Unit
$c_{b,2020}$	79	EUR/kWh
$\lambda_{b,1}$	3911	EUR/kWh
$\lambda_{b,2}$	0.3278	–
$c_{m,2020}$	2.2	EUR/kWp
$\lambda_{m,1}$	537	EUR/kWp
$\lambda_{m,2}$	0.4524	–
C_e	0.4	EUR/kWh
N_v	200 000	–
$d_{v,lf}$	200 000	km
k_{oh}	0.5350	–
C_g	14 736	EUR

Table 2
Parameters from sets $\mathcal{V}$, $\mathcal{P}$, $\mathcal{W}$ [53,55].

Tesla	Model S	Model 3	Model X	Model Y	Unit
m_g	1105	1069	1328	1205	kg
η_{gb}	0.98	0.98	0.98	0.98	–
η_{inv}	0.96	0.96	0.96	0.96	–
A_f	2.34	2.2	2.59	2.66	m^2
c_d	0.24	0.23	0.24	0.23	–
r_w	0.3518	0.3353	0.3759	0.3560	m
c_r	0.007	0.007	0.007	0.007	–
m_p	0	0	500	500	kg
m_d	80	80	80	80	kg
P_{aux}	500	500	500	500	W
$\bar{t}_a$	3.3	6.1	3.9	6.9	s
$\underline{v}_f$	100	100	100	100	km/h
$\underline{v}_t$	261	225	262	217	km/h
$\underline{v}_m$	10	10	10	10	km/h
$\underline{\theta}$	25	25	25	25	%
$\underline{d}_r$	460	405	455	350	km
w	0.25	0.25	0.25	0.25	–

3. Results

In this section, we showcase our methodology with a benchmark design problem considering the family design of four different Tesla models: Model S, Model 3, Model X and Model Y. We compare the results of the concurrent strategy with the leading technique applied in the literature and on the market, consisting in optimizing the vehicle's design specifically to minimize its own TCO, whereby the components' sizes are optimized individually for the single vehicle. However, by comparing Table 3 with Table A.7, we observe minor differences between the vehicle-tailored design and the actual commercial vehicle design. These differences can be ascribed to uncertainties in the models (we do not have access to the exact Tesla efficiency maps) and other company strategic decisions.

The vehicle-tailored design is computed with the same framework considering only one vehicle at the time, with $N_b = 1$ and $N_m = 2$ (AWD topology). In order to minimize the errors owing to market fluctuations, we adjusted the figures for inflation [76] and converted the dollars into euros where necessary [77]. In our analyses, we refer to market and technology from the year 2020. Table 1 gathers the parameters used for the cost model, Table 4 shows the reference parameters of the modules, whereas Table 2 contains vehicle parameters, performance parameters, and vehicle type fractions.

We consider the Class 3 Worldwide harmonized Light-duty vehicles Test Procedure (WLTP) for the speed and acceleration trajectories and we discretize Problem 1 using the forward Euler method with a sampling time of 1 s. Thereafter, we parse it with YALMIP [81] and solve it to global optimality with MOSEK [82], in 2 s for each of the possible N_c combinations (Fig. 6). It is important to underline that the solution depends on the sets $\mathbb{M}$ and $\mathbb{B}$. In fact, they influence the possible ratios of motor power and battery capacity among the vehicles, thus potentially increasing efficiency and lowering costs. Also, having more elements in the sets means a higher number of possible configurations, therefore increasing the total computation time.

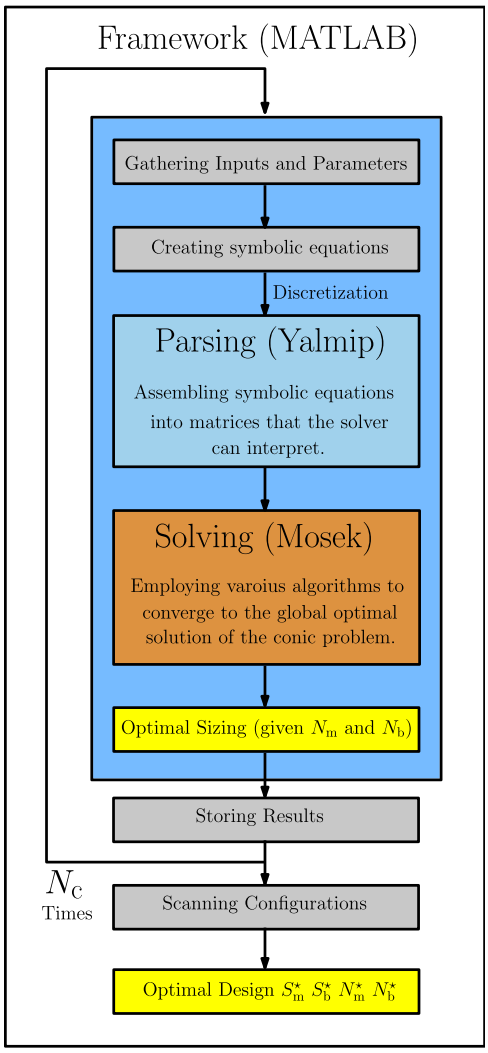

Fig. 6. Flowchart of the solution process.

Finally, in our benchmark problem, we consider equal fractions of vehicles of the ith type, i.e., $w_i = 25\%$, giving the same importance to every vehicle type. However, we perform a sensitivity analysis of the influence of this parameter on the vehicles' and family's TCO in Appendix C.

Fig. 7 shows the comparison of the TCO achieved by concurrent and tailored design optimization for an energy price 40 EUR cents per kWh, and 200 thousand vehicles, highlighting that sizing the powertrain modules for the benchmark problem using a concurrent design optimization approach achieves a reduction of the Family TCO of 3.5% compared to the individual vehicle-tailored optimization. Specifically, there is an advantageous trade-off in using standardized modules to significantly reduce the cost of manufacturing while observing a limited increase in the operation costs thanks to the higher versatility prompted by modularity. The vehicle price reduction is caused by the asymptotic relation linking the cost of an item and its production volume ((14) and (16)). For small volumes, the increase in the total amount of items caused by sharing the module features a significant item cost reduction.

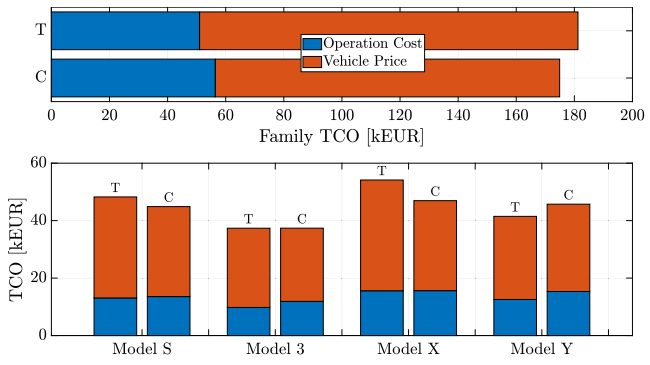

Fig. 7. Comparison of costs between the concurrent design optimization (C) and the individual vehicle-tailored design (T). The bars on the top of the picture depict the overall TCO of the family, showing a slight increment in operation cost against a significant reduction of the vehicle selling price. Below we show the single contribution of each vehicle.

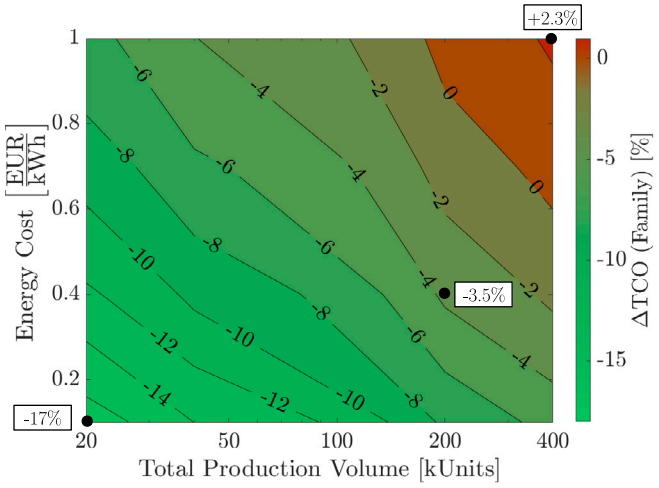

Fig. 8. Profitability map of the concurrent design optimization approach for different market conditions of energy prices and production volumes. It is especially beneficial to share family-optimal modules for cheap energy prices and for small-scale production volumes.

Conversely, for large volumes, the percentual cost reduction owing to the component sharing is smaller. For this reason, it may not keep pace with the increase in operation costs compared to the individual design. In summary, although the traditional vehicle-tailored design converges to a more energy-efficient solution since the powertrain components are specifically optimized for that vehicle, the concurrent design optimization methodology produces a family design which is overall cheaper when considering the TCO, thanks to the module cost reduction owing to the standardization and the EoS. When co-designing a large number of vehicles with very different performance constraints, some could present a higher TCO compared to the (individual) vehicle-tailored design. In fact, whilst always beneficial to the manufacturer, the family-optimal design could be disadvantageous to some users, ending up with a higher TCO compared to its vehicle-tailored design if it leads to a greater cost reduction for the rest of the family (Model Y in Fig. 7). However, as long as the overall family TCO is lower, this strategy could be exploited to shift some of the costs from economy to luxury segments where a small increase in price would put less weight on the customers' choice. Table 3 reports the family design and performance specification of the concurrent design optimized family compared to its vehicle-tailored counterpart.

Table 3
Benchmark problem family design specifications compared to a vehicle-tailored design.

Tesla	Model S	Model 3	Model X	Model Y	Unit
j_{TCO}	44 884	37 381	46 950	45 730	EUR
Δ	−6.98	+0.04	−13.28	+10.22	%
m	2232	1784	2455	2142	kg
Δ	+6.57	+7.57	+0.60	+16.31	%
d_r	533	405	462	471	km
Δ	+15.88	0.00	+1.66	+34.62	%
t_a	3.28	4.96	3.90	6.38	s
Δ	−0.71	−18.72	0.00	−7.60	%
v_t	436	359	422	337	km/h
Δ	+2.39	+9.79	+0.20	+7.97	%
F_v	0.6101	0.5354	0.7031	0.6903	MJ/km
Δ	+3.66	+21.61	+0.24	+22.13	%
$\overline{P}_{tot}$	625	313	625	313	kW
Δ	+7.33	+32.33	+0.60	+25.87	%
$\overline{E}_{tot}$	113	75	113	113	kWh
Δ	+20.12	+21.61	+1.91	+64.42	%
S_m		2.33 (312 kW)			–
Δ	+7.33	+164.67	+0.60	+151.75	%
S_b		1.60 (37.64 kWh)			–
Δ	−59.96	−39.20	−66.03	−45.19	%
N_m	2	1	2	1	–
Δ	0	−50	0	−50	%
N_b	3	2	3	3	–
Δ	+200	+100	+200	+100	%

We examine the sensitivity of the solution to different market conditions like energy price and production volume in Fig. 8. We consider electricity prices for household consumers in line with the statistics in the Netherlands [78,79] and other European countries [80]. The electricity price linearly influences the operation cost, increasing the profitability of the concurrent design optimization methodology for affordable energy, whereby this strategy leverages a trade-off between energy efficiency and component costs. Furthermore, the relative profitability of the concurrent optimization methodology grows with decreasing production volumes up to a maximum theoretical limit, achieved for 1 unit per type produced. Since the absolute saving in production cost grows asymptotically with production volumes (law of diminishing returns), the maximum theoretical limit does not have a practical application. Therefore, in Fig. 8 we show typical production volumes of electric vehicle manufacturers from data of the latest years [83]. Hence, on the one hand, employing a shared modular design is always advantageous for the vehicle manufacturer, who aims to produce as much as possible to leverage the cost reduction fostered by the EoS. On the other hand, the final user of the vehicle will benefit from a reduction in the acquisition price, which outweighs the increment in operation costs of a sub-optimal energy-efficiency family design. Above a certain threshold, depending on the production volumes, this trade-off is no longer beneficial, and an individual vehicle-tailored design is more favorable. Thus, the concurrent design methodology proves to be especially beneficial for small production volumes, becoming less and less advantageous for growing volumes, until the point where all the benefit gained from sharing the modules among the family is lost to compensate for the increase in cost of operation caused by the suboptimal energy-efficiency. Likewise, having cheap electricity prices favors the "one size fits all" approach, lowering the significance of the cost of operation term.

Table 4
Reference motor and battery parameters.

Symbol	Value	Unit
$\mathbb{M}$	$\{1,2\}$	–
$\overline{S}_{\mathrm{m}}$	4	–
$\underline{S}_{\mathrm{m}}$	0.25	–
γ	9.01	–
$m_{\mathrm{m,o}}$	81.6	kg
$\overline{P}_{\mathrm{m,o}}$	134.08	kW
ω_{r}	490.58	rad/s
r_{FWD}	0.6	–
r_{AWD}	1	–
$\mathbb{B}$	$\{1,2,3\}$	–
$\overline{S}_{\mathrm{b}}$	4	–
$\underline{S}_{\mathrm{b}}$	0.25	–
$m_{\mathrm{b,o}}$	138.6	kg
$\overline{E}_{\mathrm{b,o}}$	23.48	kWh
$\overline{\xi}$	0.9	–
$\underline{\xi}$	0.1	–

4. Conclusions

This paper presented a concurrent design optimization framework to identify the optimal size and multiplicity of motor and battery modules that are installed within a family of electric vehicles, explicitly accounting for Economy of Scale (EoS) effects on the resulting Total Cost of Ownership (TCO). To this end, we devised a cost model capturing the influence of production volumes, energy cost, modules' size and multiplicity on the vehicle's TCO, and a powertrain model to account for its operations. The resulting framework enables to compute minimum-TCO vehicle family design solutions with global optimality guarantees. When applied to a real-world case study for the design of the Tesla vehicle family, our methodology achieves a reduction of 3.5% in the family TCO compared to vehicle-tailored design solutions, whilst maintaining a comparable level of performance. We showed that the profitability of the approach ranges from a reduction in family TCO of 17% for cheap energy prices and small production volumes to an increase of 2.3% for very expensive energy prices and large production volumes. Even so, the approach is always beneficial to the vehicle manufacturer as it minimizes the production cost at the expense of the vehicles' energy efficiency, while not requiring any particular cost investments. Overall, concurrent design optimization proved to be advantageous for a wide range of volumes and electricity prices, creating an opportunity to support the transition to electric mobility by substantially reducing the vehicle's upfront cost, one of the major factors hindering its adoption.

This work opens the field for the following extensions: First, we aim to sophisticate the framework by incorporating the optimization of the transmission and more powertrain architectures. Second, we would like to assess the vehicles' environmental impact via life cycle analysis and study the effect of its minimization on the design solutions.

CRediT authorship contribution statement

Maurizio Clemente: Writing – review & editing, Writing – original draft, Visualization, Validation, Software, Resources, Project administration, Methodology, Investigation, Formal analysis, Data curation, Conceptualization. **Mauro Salazar:** Writing – review & editing, Supervision. **Theo Hofman:** Writing – review & editing, Supervision, Funding acquisition.

Declaration of competing interest

The authors declare that they have no known competing financial interests or personal relationships that could have appeared to influence the work reported in this paper.

Acknowledgments

The authors would like to thank Ir. O. J. T. Borsboom, F. Vehlhaber, F. Paparella, Dr. D. Herceg, and Dr. I. New for proofreading this paper.

Appendix A. Cost model

After a careful review of the literature, we developed a cost model able to portray the influence of EoS strategies on battery packs and motor costs. We report the data [43,44,66,67,84,85] used to identify $c_{\mathrm{b},2020}$, $\lambda_{\mathrm{b},1}$, $\lambda_{\mathrm{b},2}$, $c_{\mathrm{m},2020}$, $\lambda_{\mathrm{m},1}$, and $\lambda_{\mathrm{m},2}$ in Table A.6, portraying the identified functions in Figs. A.9 and A.10. Furthermore, we indicate the glider cost depending on the vehicle type in Table A.5. Finally, we compute the selling price from the manufacturing cost by considering the overhead costs to be a constant fraction [47] k_{oh}, as shown in Fig. A.12. The prediction of the cost model has been validated with a set of different BEVs, achieving good results in modeling vehicle price using just the vehicle type, battery capacity, and motor power, assuming an average hundred thousand vehicles produced (Table A.7 and Fig. A.11). However, the error in the prediction increases for luxury brands, where the price is heavily influenced by factors which are not strongly coupled with manufacturing.

Table A.5
Glider costs in 2020 [42,51].

Vehicle type	Glider cost [EUR]
City cars	7996
Compact cars	10 779
Large cars	14 736

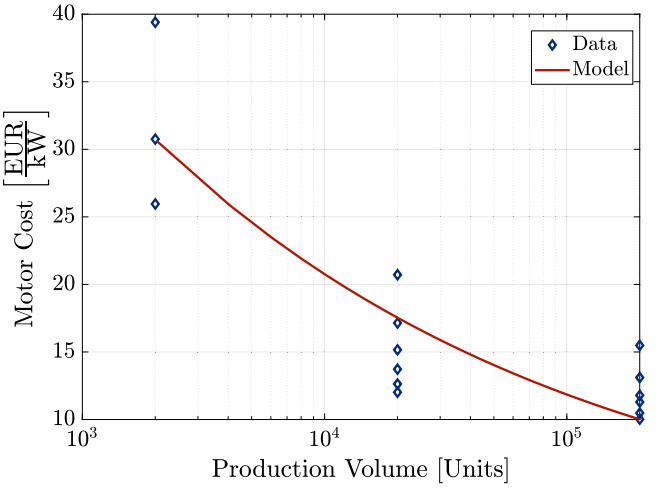

Fig. A.9. Production volumes impact on the motor cost in Euro per kW.

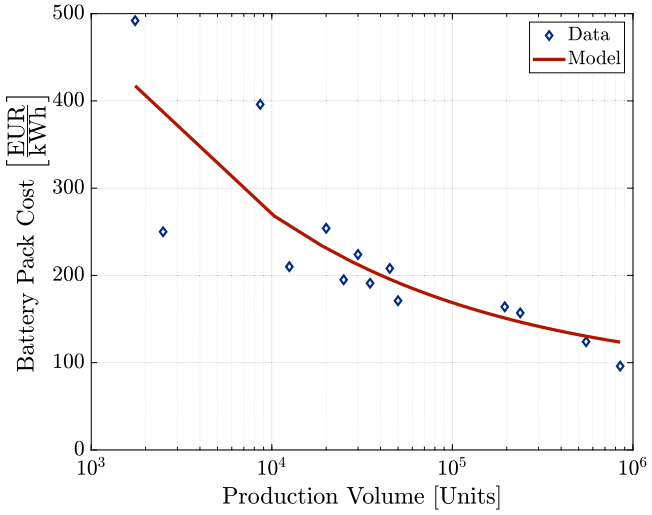

Fig. A.10. Production volumes impact on the battery pack cost in Euro per kWh.

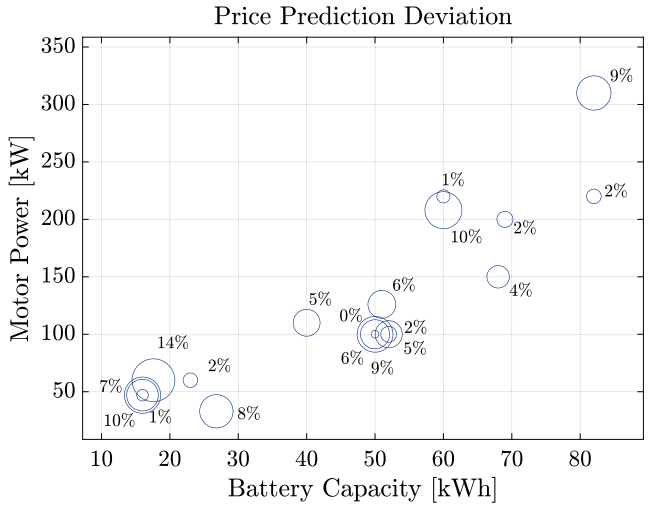

Fig. A.11. Percentage deviation of the model prediction from vehicles' price.

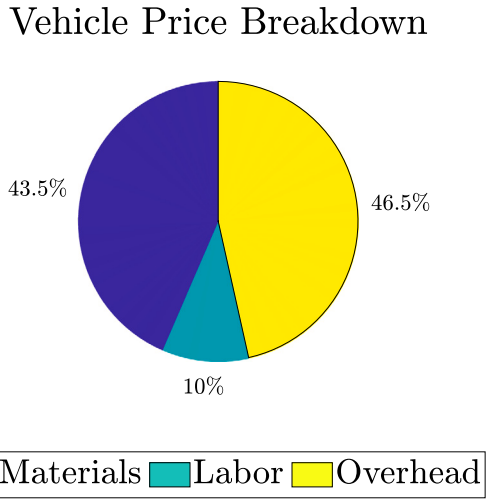

Fig. A.12. Price breakdown of a new vehicle [47,63].

Table A.6
Peak-power-specific cost by production volumes [48,49] (left), and Battery Pack capacity-specific cost by production volumes [46,47,50] (right).

Motor Units	Cost [EUR/kW(p)]	Battery pack Units	Cost [EUR/kWh]
2000	39.40	1750	492
2000	30.75	2500	250
2000	25.95	8625	396
20 000	20.71	12 500	210
20 000	17.14	20 000	254
20 000	15.15	25 000	195
20 000	13.72	30 000	224
20 000	12.62	35 000	191
20 000	12.01	45 000	208
2 00 000	15.48	50 000	171
2 00 000	13.10	95 000	164
2 00 000	11.78	237 500	157
2 00 000	11.29	550 000	124
2 00 000	10.47	850 000	96
2 00 000	10.02		

Table A.7
Validation of the vehicle's cost model assuming an average production volume of a hundred thousand vehicles per type.

Vehicle	Capacity kWh	Power kW	Pred. EUR	Price EUR
City (Seg. A-B)				
Mitsubishi i-MiEV	16	47	20 188	19 990 [54]
Peugeot iOn	16	47	20 188	22 360 [86]
Citroen C-Zero	16	47	20 188	21 800 [86]
Smart EQ fortwo	17.6	60	20 746	23 995 [86]
Renault Twingo E	23	60	22 450	22 105 [56]
Dacia Spring El.	26.8	33	23 537	21 750 [57]
Opel Corsa-e	50	100	31 134	30 999 [58]
Peugeot e-208	50	100	31 134	33 220 [59]
Renault Zoe Q90	52	100	31 765	33 590 [86]
Compact (Seg. C)				
Nissan Leaf	40	110	33 222	35 090 [86]
Citroen e-C4 X	50	100	36 336	40 140 [87]
ORA Funky Cat	51	126	36 758	38 990 [86]
Renault Zoe R135	52	100	36 967	36 295 [86]
Kia Niro EV	68	150	42 221	43 850 [60]
Large (Seg. D-E)				
Tesla Model 3	60	208	47 333	42 993 [53]
Tesla Model Y	60	220	47 382	47 993 [53]
Polestar 2	69	200	50 222	51 200 [61]
Polestar 2 LR	82	220	54 324	55 200 [61]
Polestar 2 Dual LR	82	310	54 695	59 900 [61]

Appendix B. Powertrain component models

The motor and the battery models capture the susceptibility of the efficiency to the components' sizing and the different dynamic driving conditions determined by the cycle D, according to the equations presented in Sections 2.3.4 (Motor) and 2.3.5 (Battery). We show the identified motor parameters of Eq. (22), namely $P_0(\omega)$, $\beta(\omega)$ and $\alpha(\omega)$, in Fig. B.13, resulting in the efficiency map from Fig. B.14, with a normalized root mean square error (NRMSE) of 0.41% on the efficiency. Likewise, the battery losses depend on the function P_{sc} presented in Eq. (26), which is also determined through a parameter identification process on the reference component, with an NRMSE of 1.32% on P_{sc}.

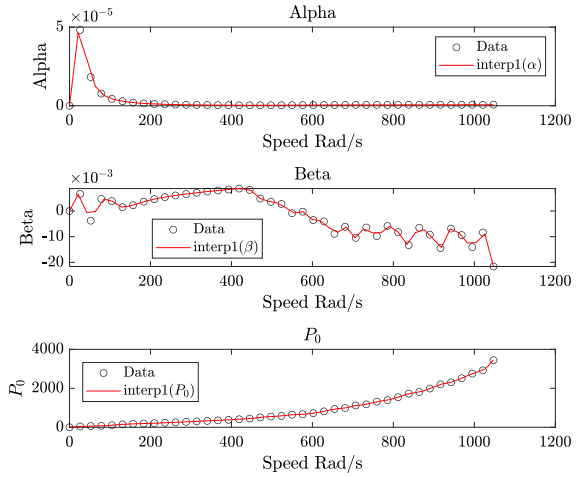

Fig. B.13. Speed-level dependent identified motor loss coefficients.

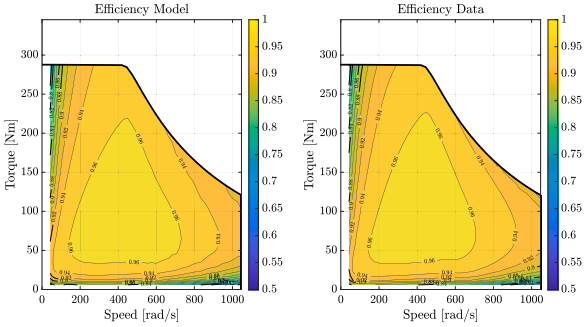

Fig. B.14. Reference electric motor efficiency map from the model (left) compared with data (right).
Source: Data from [39].

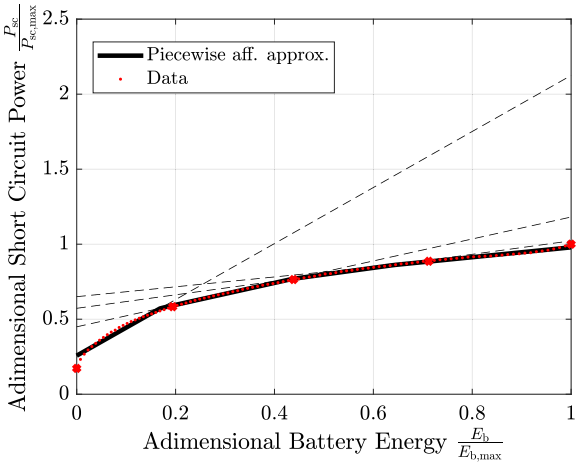

Fig. B.15. Reference battery short circuit power as a function of the battery energy. The slope and the intercept of the piecewise affine approximations are the battery loss coefficients a_k and b_k.

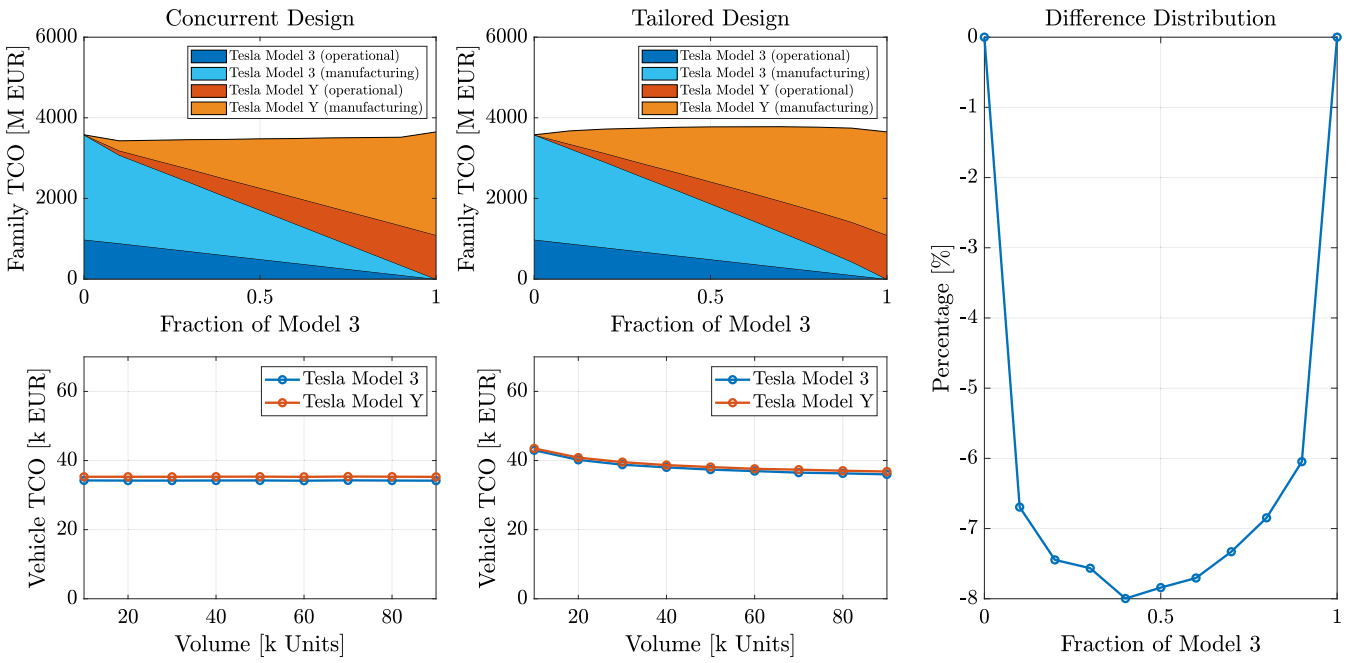

Fig. C.16. Sensitivity analysis of Tesla Model 3 and Tesla Model Y with respect to the vehicle type fraction w_i and a total production of 100 000 units. For fractions 0 or 1, one of the vehicles is not produced while the other is optimized individually.

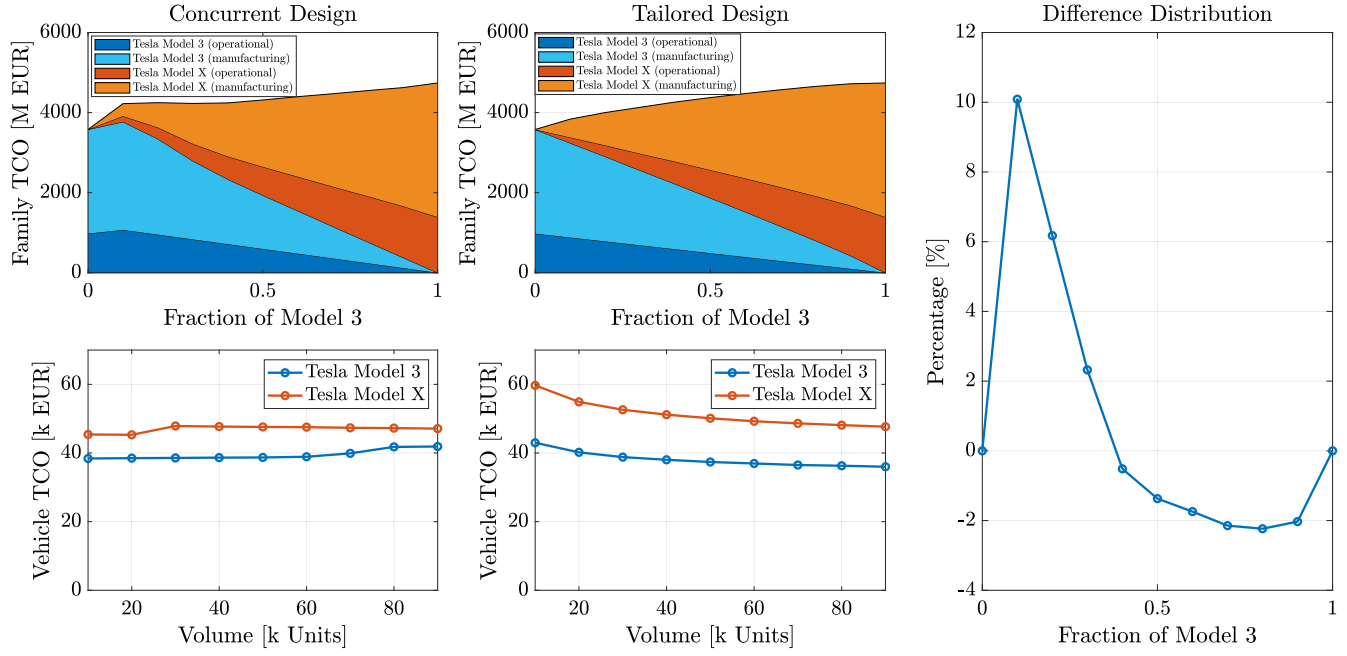

Fig. C.17. Sensitivity analysis of Tesla Model 3 and Tesla Model X with respect to the vehicle type fraction w_i and a total production of 100 000 units. For fractions 0 or 1, one of the vehicles is not produced while the other is optimized individually.

The slope and the intercept of the piecewise affine approximations of P_{sc} presented in Fig. B.15 are the battery loss coefficients a_k and b_k, respectively, from Eq. (25). Finally, in line with common practices in the field [24], we assumed the gearbox and inverter efficiencies constant since the impact of different operative conditions on their efficiency is lower compared to other powertrain components, such as motor and battery.

Appendix C. Vehicle type fraction sensitivity analysis

We analyze the sensitivity of the solution to the vehicle type fraction w_i, adjusting the ratio by 1/10 increments each time. In the concurrent design optimization strategy, if the vehicles are similar enough to share the same powertrain, each vehicle's TCO depends on the total production volume, regardless of the specific production volume of each vehicle. Conversely, using a vehicle-tailored design leads to different costs that depend on each vehicle's individual production volume.

As a matter of fact, in the scenario shown in Fig. C.16, the benefit of sharing a modular powertrain peaks around an approximately equal production fraction (though this depends on the respective costs of the vehicles), as an equal fraction does not significantly reduce the costs of any individual vehicle in a vehicle-tailored design.

When applying the concurrent design optimization strategy to vehicles that differ significantly and thus have different modularity of components (Fig. C.17), an uneven fraction could result in more expensive designs compared to a vehicle-tailored approach. In fact, the smaller fraction could constrain the larger segment to adopt an oversized powertrain, increasing both component costs and energy consumption.

Data availability

No data was used for the research described in the article.

References

[1] IEA. Global EV outlook 2021. Technical report, International Energy Agency; 2021.
[2] McTurk E. Do electric vehicles produce more tyre and brake pollution than petrol and diesel cars? Technical report, Plug Life Consulting for the RAC; 2022.
[3] IEA. Global EV outlook 2020. Technical report, International Energy Agency; 2020.
[4] UNEP, DTU. Emissions gap report 2021: The heat is on – A world of climate promises. Technical report, United Nations Environment Programme and Technical University of Denmark; 2021.
[5] IEA. Global EV outlook 2022. Technical report, International Energy Agency; 2022.
[6] Paoli L. Electric cars fend off supply challenges to more than double global sales. Paris; 2022, https://www.iea.org/commentaries/electric-cars-fend-off-supply-challenges-to-more-than-double-global-sales.
[7] Avicenne Energy. European union and UK automotive ICE vs EV total cost of ownership. Technical report, Nickel Institute; 2021.
[8] Lightyear. Producing worldś most efficient car to date, under every weather condition and speed. 2022, https://lightyear.one/articles/producing-worlds-most-efficient-car-to-date-under-every-weather-condition-and-speed, Online.
[9] Medini K, Pierné A, Erkoyuncu JA, Cornet C. A model for cost-benefit analysis of production ramp-up strategies. In: Lalic B, Majstorovic V, Marjanovic U, von Cieminski G, Romero D, editors. Proc. of advances in production management systems. Springer International Publishing; 2020, p. 731–9.
[10] Advanced Manufacturing Office. Improving motor and drive system performance. Technical report, US Department of Energy: Energy Efficiency & Renewable Energy; 2014.
[11] Jiao J, Simpson TW, Siddique Z. Product family design and platform-based product development: a state-of-the-art review. J Intell Manuf 2007;18(1):5–29.
[12] Robertson D, Ulrich K. Planning for product platforms. Whart Annu 1998;39(4):19–31.
[13] Otto K, Hölttä-Otto K, Simpson TW, Krause D, Ripperda S, Moon SK. Global views on modular design research: Linking alternative methods to support modular product family structure design. ASME J Mech Des 2016;138(7):071101.
[14] Simpson TW, Siddique Z, Jiao J. Product platform and product family design methods and applications. 1st ed.. Springer US; 2006.
[15] Sanderson SW, Uzumeri M. Managing product families: The case of the Sony Walkman. Res Policy 1995;24(5):761–82.
[16] Sanderson SW, Uzumeri M. Managing product families. 2nd ed.. McGraw-Hill Publishing Co.; 1997.
[17] Sabbagh K. Twenty-first century jet: The making and marketing of the boeing 777. 1st ed.. New York, NY: Scribner; 1996.
[18] Rothwell R, Gardiner P. Robustness and product design families. In: Design management: A handbook of issues and methods. 1st ed.. Basil Blackwell Inc., Cambridge MA; 1990, p. 279–92, chapter.
[19] Caffrey RT, Simpson TW, Henderson R, Crawley E. The technical issues with implementing open avionics platforms for spacecraft. In: 40th AIAA aerospace sciences meeting. 2022.
[20] Bremmer R. Cutting-edge platforms. Final Times Automot World 1999;1999(6):30–8.
[21] Bremmer R. Big, bigger, biggest. Automot World 2000;2000(6):36–44.
[22] Nobeoka K, Cusumano MA. Thinking beyond lean: How multi-project management is transforming product development at toyota and other companies. 1st ed.. Free Press; 1997,
[23] Pereirinha PG, Trovão JP. Standardization in electric vehicles. In: 12th portuguese-spanish conference on electerical engineering. 2011.
[24] Guzzella L, Sciarretta A. Vehicle propulsion systems: Introduction to modeling and optimization. 2nd ed.. Springer Berlin Heidelberg; 2007.
[25] Silvas E, Hofman T, Murgovski N, Etman P, Steinbuch M. Review of optimization strategies for system-level design in hybrid electric vehicles. IEEE Trans Veh Technol 2016;66(1):57–70.
[26] Wang Z, Zhou J, Rizzoni G. A review of architectures and control strategies of dual-motor coupling powertrain systems for battery electric vehicles. Renew Sustain Energy Rev 2022;162(1):112455.
[27] Dong P, Zhao J, Xu X, Wang R, Lin X, Liu Y, Wang S, Guo W. Rapid assessment of series–parallel hybrid transmission comprehensive performance: A near-global optimal method. eTransportation 2023;15:100221.
[28] Kwon K, Lim S, Kim D, Park K. Automation program for optimum design of electric vehicle powertrain systems based on artificial neural network. eTransportation 2023;18:100267.
[29] Hofman T, Salazar M. Transmission ratio design for electric vehicles via analytical modeling and optimization. In: IEEE vehicle power and propulsion conference. 2020.
[30] Radrizzani S, Riva G, Panzani G, Corno M, M. SS. Optimal sizing and analysis of hybrid battery packs for electric racing cars. IEEE Trans Transp Electr 2023;1.
[31] Verbruggen FJR, Rangarajan V, Hofman T. Powertrain design optimization for a battery electric heavy-duty truck. In: Proc. of the American control conference. 2019.
[32] Borsboom O, Fahdzyana CA, Hofman T, Salazar M. A convex optimization framework for minimum lap time design and control of electric race cars. IEEE Trans Veh Technol 2021;70(9):8478–89.
[33] Da Silva DC, Kefsi L, Sciarretta A. Analytical models for the sizing optimization of fuel cell hybrid electric vehicle powertrains. In: 16th international conference on engines & vehicles. IFP Energies Nouvelles Inst. Carnot IFPEN Transports Energie; 2023, p. 0133–51.
[34] Borsboom O, Salazar M, Hofman T. Electric motor design optimization: A convex surrogate modeling approach. In: Symposium on advances in automotive control. 2022.
[35] Zhang H, Qin Y, Li X, Liu X, Yan J. Power management optimization in plug-in hybrid electric vehicles subject to uncertain driving cycles. eTransportation 2020;3:100029.
[36] Ribau JP, Silva CM, Sousa JMC. Efficiency, cost and life cycle CO2 optimization of fuel cell hybrid and plug-in hybrid urban buses. Appl Energy 2014;129:320–35.
[37] Anselma P. Electric powertrain sizing for vehicle fleets of car makers considering total ownership costs and CO_2 emission legislation scenario. Appl Energy 2022;1(314):118902.
[38] Clemente M, Salazar M, Hofman T. Concurrent powertrain design for a family of electric vehicles. In: 10th advances in automotive control. 2022.
[39] Solipuram VR. Electric and internal combustion engine powertrain models. 2024, https://www.mathworks.com/matlabcentral/fileexchange/77188-electric-and-internal-combustion-engine-powertrain-models, Central File Exchange.
[40] Hoekstra A, Vijayashankar A, Sundrani VL. Modelling the total cost of ownership of electric vehicles in the Netherlands. In: Proc. of the int. symp. on electric vehicles 30th edition. 2017.
[41] Simeu S, Kim N. Standard driving cycles comparison (IEA) & impacts on the ownership cost. In: Inpreceedings of the SAE world congress & exibition. 2018.
[42] Simeu K, Kim N, Dupont B. Bean. 2021, https://vms.taps.anl.gov/tools/bean/, Online.
[43] Fries M, Kerler M, Rohr S, Sinning M, Lienkamp M. Technical report, Technische Universität München; 2017, Update 2017.
[44] Kochhan R, Fuchs S, Reuter B, Burda P, Matz S, Lienkamo M. An overview of costs for vehicle components, fuels, greenhouse gas emissions and total cost of ownership. 2014, 2014.
[45] Brooker A, Gonder J, Wang L, Wood E, Lopp S, Ramroth L. FASTSIM: a model to estimate vehicle efficiency, cost and performance. SAE Tech Pap 2015;1:0973.
[46] Anderman M. Extract from the xEV insider report. Technical report, Total Battery Consulting; 2019.
[47] König A, Nicoletti L, Schröder D, Wolff S, Waclaw A, Lienkamp M. An overview of parameter and cost for battery electric vehicles. World Electr Veh J 2021;12(1):21–50.
[48] Lipman T. The cost of manufacturing electric vehicle drivetrains. Technical report, Univ. of California, Berkeley; 1999.
[49] Cuenca RM. Simple cost model for EV traction motors. In: Proceedings of the second world car conference, university of california at riverside. Center for Transportation Research Energy System Division Argonne National Laboratory; 1995.
[50] Philippot M, Alvarez G, Ayerbe E, Van Mierlo J, Messagie M. Eco-efficiency of a lithium-ion battery for electric vehicles: Influence of manufacturing country and commodity prices on GHG emissions and costs. Batteries 2019;5(23):17.
[51] Sabri Islam E, Vijayagopal R, Moawad A, Kim N, Dupont B, Nieto Prada D, Rousseau A. A detailed vehicle modeling & simulation study quantifying energy consumption and cost reduction of advanced vehicle technologies through 2050. Technical report, U.S. Dept. of Energy Contract ANL/ESD-21/10; 2021.
[52] Cox B, Bauer C, Mendoza Beltran A, Van Vuuren DP, Mutel CL. Life cycle environmental and cost comparison of current and future passenger cars under different energy scenarios. Appl Energy 2020;269:115021.
[53] Tesla. Tesla website. 2023, https://www.tesla.com/, Online.
[54] Autoweek. Mitsubishi I-MIEV. 2023, https://www.autoweek.nl/auto/59111/mitsubishi-i-miev/, Online.
[55] EVDatabase. Electric vehicle database. 2022, Available at https://ev-database.uk.
[56] Autoweek. Renault twingo electric collection. 2023, https://www.autoweek.nl/auto/100944/renault-twingo-electric-collection/, Online.

[57] DACIA. DACIA spring. 2023, https://www.vanmossel.nl/dacia/acties/dacia-spring/, Online.
[58] OPEL. Opel corsa-e. 2023, https://www.opel.nl/personenwagens/corsa-modellen/corsa-electric/overzicht.html, Online.
[59] Peugeot. Peugeot official website. 2023, https://www.peugeot.nl/elektrisch-en-hybride, Online.
[60] Kia. Kia niro EV pricelist. 2023, January, Online.
[61] Polestar. Polestar website. 2023, https://www.polestar.com/nl/polestar-2/specifications/, Online.
[62] Office of Energy Efficiency and Renewable Energy. United States industrial electric motor systems market opportunities assessment. Technical report, U.S. Department of Energy; 1998.
[63] WirtschaftsWoche. Zusammensetzung des preises eines neuwagens in deutschland. 2014, Online.
[64] Del Duce A, Gauch M, Althaus HJ. Electric passenger car transport and passenger car life cycle inventories in ecoinvent version 3. Int J Life Cycle Assess 2014;2014(21):1314–26.
[65] Barnes I. Automotive gearbox overhaul manual. 1st ed.. Haynes Manuals Inc.; 1998.
[66] Rajashekara K, Martin R. Electric vehicle propulsion systems present and future trends. J Circuits Syst Comput 1995;5(1):109–219.
[67] Vyas A, Cuenca R, Gaines L. An assessment of electric vehicle life cycle cost to consumers. SAE Tech Pap 1998;982182.
[68] Verbruggen FJR, Salazar M, Pavone M, Hofman T. Joint design and control of electric vehicle propulsion systems. In: European control conference. 2020.
[69] Ebbesen S, Salazar M, Elbert P, Bussi C, Onder CH. Time-optimal control strategies for a hybrid electric race car. IEEE Trans Control Syst Technol 2018;26(1):233–47.
[70] Murgovski N, Johannesson L, Sjöberg J, Egardt B. Component sizing of a plug-in hybrid electric powertrain via convex optimization. Mechatronics 2012;22(1):106–20.
[71] Aroua A, Lhomme W, Verbelen F, Ibrahim MN, Bouscayrol A, Sergeant P, Stockman K. Impact of scaling laws of permanent magnet synchronous machines on the accuracy of energy consumption computation of electric vehicles. eTransportation 2023;18:100269.
[72] Simon B, Weil M. Analysis of materials and energy flows of different lithium ion traction batteries. Rev Metall 2013;(110):65–76.
[73] Tagliaferri C, Evangelisti S, Acconcia F, Domenech T, Ekins P, Barletta D, Lettieri P. Life cycle assessment of future electric and hybrid vehicles: A cradle-to-grave systems engineering approach. Chem Eng Res Des 2016;(112):298–309.
[74] Ellingsen LA, Singh B, Strømman AH. The size and range effect: lifecycle greenhouse gas emissions of electric vehicles. Environ Res Lett 2016;11:054010.
[75] Boyd SP, Wegbreit B. Fast computation of optimal contact forces. IEEE Trans Robot Autom 2007.
[76] Alioth Finance. Inflation calculator 1 dollar in 1991 to 2022. 2022, https://www.officialdata.org/us/inflation/1991?amount=1, Online.
[77] Google Finance. USD/EUR conversion. 2022, Available: https://www.google.com/finance/quote/USD-EUR?hl=en&window=1M, Online.
[78] Ministry of Economic Affairs and Climate Policy. Price cap for gas, electricity and district heating. 2023, Online. [Acccessed 19 September 23].
[79] Centraal Bureau voor de Statistiek. Average energy prices for consumers 2018–2023. 2023, Online. [Accessed 04 August 2023].
[80] Eurostat. Electricity prices for households in the European Union (EU-27/EU-28) from 1st half 2010 to 1st half 2022 (in euro cents per kilowatt-hour). 2022, Available: https://www.statista.com/statistics/418049/electricity-prices-for-households-in-eu-28/, Online.
[81] Löfberg J. YALMIP : A toolbox for modeling and optimization in MATLAB. In: IEEE int. symp. on computer aided control systems design. 2004.
[82] MOSEK ApS. MOSEK optimization software. 2017, Available at https://mosek.com/.
[83] Tesla. Number of Tesla vehicles produced worldwide from 1st quarter 2016 to 2nd quarter 2023 (in units). 2023, www.statista.com/statistics/715421/tesla-quarterly-vehicle-production/, Online.
[84] Office of Technology Assessment. Advanced automotive technology: Visions of a super-efficient family car. Princeton; 1995,
[85] de Santiago J, Bernhoff H, Ekergard B, Eriksson S, Ferhatovic S, Waters R. Electrical motor drivelines in commercial all electric vehicles: a review. Trans Veh Techonol 2012;61(2):475–84.
[86] Elektrische Voertuigen Database. EV database. 2023, v4.4, Online.
[87] CITROEN. Prijslist. 2023, www.citroen.nl/content/dam/citroen/netherlands/b2c/local-content/brochures-prijslijsten/model/c4/consumentenprijslijst-e-c4.358875.pdf, Online.